

Plastic wave propagation in Hopkinson bar - revisited

M. MIĆUNOVIĆ⁽¹⁾ and A. BALTOV⁽²⁾

⁽¹⁾ *Faculty of Mechanical Engineering, University of Kragujevac,
Sestre Janjica 6a, 34000 Kragujevac, Yugoslavia
e-mail: mmicun@EUnet.yu*

⁽²⁾ *Institute of Mechanics, Bulgarian Academy of Sciences
bl. 4, Acad. G. Bontchev str., 1113 Sofia, Bulgaria
e-mail: baltov@imbm.bas.bg*

*Dedicated to Professor Piotr Perzyna
on the occasion of his 70th birthday*

THE SUBJECT OF this paper is an analysis of the experimental Hopkinson bar technique when such a device consists of a short tensile or shearing specimen surrounded by two very long elastic bars [1]. Unlike the commonly applied by-pass analysis which attempts to draw conclusions from the behaviour of elastic bars, we attempt to take into account real plastic waves inside the specimen with several hundreds of reflections. A quasi rate-independent as well as a more general, rate-dependent tensor function model for AISI 316H calibrated in [19] are applied. Some special slightly perturbed elastic incident and reflected waves in elastic bars served to simulate the starting solutions. The numerical results have shown a good agreement with experimentally observed homogeneous strain state throughout the specimen during the process. Lindholm's procedure for finding specimen stress and strain by such a by-pass procedure is criticized.

1. Introduction

THE GOAL of this paper is to revisit the standard techniques for analysis of the Hopkinson bar testing technique, taking into account plastic wave propagation inside the standard (extremely short) tension specimen, as well as elastic waves propagating along the very long incident-reflected wave bar and the transmitted wave bar. The strains inside the specimen are large and reach up to 60%. The evolution equation for plastic stretching tensor was calibrated in [19] on the basis of the experiments performed in dynamic testing laboratory of the JRC-Ispra, Italy [1, 2, 3], with classical tension specimen as well as "bichierrino" shear specimen (consisting of two rigid cylinders connected by the gauge part - a thin circular crown explained in detail in [4]) made of austenitic stainless steel AISI 316H, in the range of strain rates $[10^{-3}, 10^3]s^{-1}$.

2. Preliminaries

Before proceeding, clear stress and strain measures are necessary. It is commonly accepted that in addition to the undeformed configuration \mathcal{B}_0 and the instant deformed configuration \mathcal{B} , an intermediate local reference configuration \mathcal{B}_N is introduced. Then Kroener's decomposition rule holds [9]

$$(2.1) \quad \mathbf{F} = \mathbf{F}_E \mathbf{F}_P$$

where \mathbf{F} – the deformation gradient tensor, \mathbf{F}_E – the elastic distortion tensor, and \mathbf{F}_P – the plastic distortion tensor, mapping respectively $\mathcal{B}_0 \rightarrow \mathcal{B}$, $\mathcal{B}_N \rightarrow \mathcal{B}$ and $\mathcal{B}_0 \rightarrow \mathcal{B}_N$. The name “distortion” is used to underline the fact that \mathbf{F}_E and \mathbf{F}_P are incompatible, i.e. compatibility conditions applied to a metric tensor of \mathcal{B}_N are not satisfied (cf. e.g. [13]). Let us apply polar decomposition on plastic distortion i.e. $\mathbf{F}_P = \mathbf{R}_P \mathbf{U}_P = \mathbf{V}_P \mathbf{R}_P$, where \mathbf{R}_P is the plastic rotation tensor \mathbf{U}_P and \mathbf{V}_P are the right and the left plastic stretch tensors. In the subsequent sections it will be especially convenient to use logarithmic plastic strain by making use of the definition:

$$(2.2) \quad \mathbf{e}_P = \ln \mathbf{V}_P = \frac{1}{2} \ln (\mathbf{F}_P \mathbf{F}_P^T).$$

It is traceless when plastic volume change is negligible (which takes place whenever damage such as creep, low-cycle-fatigue, irradiation creep etc. is not taken into account). It is worth of note that this holds true for large plastic strains as well. As another strain measure, the Lagrangean elastic strain will be used

$$(2.3) \quad \mathbf{E}_E = \frac{1}{2} (\mathbf{F}_E^T \mathbf{F}_E - \mathbf{1}).$$

Both measures are referred to the vectorial base vectors of \mathcal{B}_N . Another tensor connected also with the configuration \mathcal{B}_N , being of importance for the following considerations, is the plastic stretching tensor:

$$(2.4) \quad \mathbf{D}_P = \frac{1}{2} (\dot{\mathbf{F}}_P \mathbf{F}_P^{-1} + \mathbf{F}_P^{-T} \dot{\mathbf{F}}_P^T),$$

where the superposed dot stands for material differentiation with respect to time holding considered particle fixed.

According to the assumption that the elastic strain is caused and escorted by the corresponding stress tensor, Hooke's law holds for the mapping $\mathcal{B}_N \rightarrow \mathcal{B}$ and it should be written in an invariant way connected with the intermediate referential configuration \mathcal{B}_N . For this aim, aside stress tensor present in \mathcal{B} – configuration, called Cauchy stress (or “true” stress), we quote also the first and second Piola-Kirchhoff stress tensor [28]:

$$(2.5) \quad \mathbf{T}_R = \det(\mathbf{F}) \mathbf{T} \mathbf{F}^{-T}, \quad \mathbf{S} = \det(\mathbf{F}_E) \mathbf{F}_E^{-1} \mathbf{T} \mathbf{F}_E^{-T},$$

respectively. The first of them is connected with \mathcal{B} and \mathcal{B}_0 and often it is named the engineering stress, whereas the second one is referred to the natural state local configuration \mathcal{B}_N . If the elastic strain is much smaller than the finite total strain, then Hooke's law reads:

$$(2.6) \quad \mathbf{S} = \mathcal{H} : \mathbf{E}_E.$$

Fourth rank tensor \mathcal{H} consisting of material constants should depend in general on temperature as well as on principal invariants of the (traceless) plastic strain tensor.

$$(2.7) \quad \pi_2 = tr \{ \mathbf{e}_P^2 \}, \quad \pi_3 = tr \{ \mathbf{e}_P^3 \}.$$

Two basic tensor constituents of the subsequent evolution equations are the plastic strain tensor and the second Piola-Kirchhoff stress tensor defined above. Thus, the relevant tensor generators are (the subscript d is used to denote the deviatoric part of a second rank tensor) [28, 21]:

$$(2.8) \quad \begin{aligned} \mathbf{H}_1 &= \mathbf{S}_d, \quad \mathbf{H}_2 = (\mathbf{S}_d^2)_d, \quad \mathbf{H}_3 = \mathbf{e}_P, \quad \mathbf{H}_4 = (\mathbf{e}_P^2)_d, \\ \mathbf{H}_5 &= (\mathbf{S}_d \mathbf{e}_P + \mathbf{e}_P \mathbf{S}_d)_d, \quad \mathbf{H}_6 = (\mathbf{S}_d \mathbf{e}_P^2 + \mathbf{e}_P^2 \mathbf{S}_d)_d, \\ \mathbf{H}_7 &= (\mathbf{S}_d^2 \mathbf{e}_P + \mathbf{e}_P \mathbf{S}_d^2)_d, \end{aligned}$$

while the corresponding principal and mixed invariants will also be necessary in the sequel:

$$(2.9) \quad \begin{aligned} s_2 &= tr (\mathbf{S}_d^2), \quad s_3 = tr (\mathbf{S}_d^3), \quad \mu_1 = tr (\mathbf{S}_d \mathbf{e}_P), \\ \mu_2 &= tr (\mathbf{S}_d \mathbf{e}_P^2), \quad \mu_3 = tr (\mathbf{S}_d^2 \mathbf{e}_P), \quad \mu_4 = tr (\mathbf{S}_d^2 \mathbf{e}_P^2), \\ \gamma &\equiv \{ s_2, s_3, \pi_2, \pi_3, \mu_1, \mu_2, \mu_3, \mu_4 \}. \end{aligned}$$

As usual, some of the above principal invariants are used here to denote the intensities of the corresponding tensors

$$(2.10) \quad S = \sqrt{s_2}, \quad \dot{\pi} = (\mathbf{D}_P : \mathbf{D}_P)^{1/2}, \quad \pi = \int_0^\tau \dot{\pi}(\tau') d\tau'.$$

In the terminology of experimental plasticity, in a slightly different form

$$(2.11) \quad \sigma^{eq} = S \sqrt{\frac{3}{2}}, \quad \varepsilon_P^{eq} = \dot{\pi} \sqrt{\frac{2}{3}}, \quad \dot{\varepsilon}_P^{eq} = \pi \sqrt{\frac{2}{3}},$$

they are commonly named *equivalent stress*, *equivalent plastic strain* (i.e. accumulated plastic strain) and *equivalent plastic strain rate*.

3. Experimental evidence and evolution equations

It has been known by experimentalists for a long time that initial yield stress depends on the strain rate or on the stress rate such that at higher stress rates, initial yield stress is larger. On the other hand, Rabotnov in his book has suggested that there exists the phenomenon of delayed yielding inherent at some metals and alloys, i.e. it means that stress exceeds its static value after elapsing of a certain time interval called the delay time. According to such an assumption, in the paper [19] the following integral equation

$$(3.1) \quad \pi(\tau) = \int_0^\tau J(\tau - \tau') \frac{DS(\tau')}{D\tau'} d\tau' \equiv \int_0^\tau \psi(\tau, \tau') d\tau'$$

was postulated and calibrated.

If plastic deformation commences at time τ^* so that initial stress time rate equals

$$(3.2) \quad S(\tau^*) \equiv Y_0 \left(\frac{DS(\tau)}{D\tau} \Big|_{\tau=\tau^*} \right),$$

then the initial yield stress depends on the initial time rate of stress. Accordingly, the kernel in the above integral equation should read

$$(3.3) \quad J(\tau - \tau') = \begin{cases} 0, & \tau < \tau^*, \\ \exp(-\mathcal{M}), & \tau \geq \tau^*. \end{cases}$$

Applying this expression for kernel to the above integral equation, the following representation is acquired:

$$(3.4) \quad \dot{\pi}(\tau) = J(0) \frac{DS(\tau)}{D\tau} = \begin{cases} 0, & \tau < \tau^*, \\ \exp(-\mathcal{M}) \sqrt{2/3} \dot{\sigma}^{eq}(\tau), & \tau \geq \tau^*. \end{cases}$$

The integral appearing in (3.1) is the Riemann integral. Indeed, it is not difficult to show that it is uniformly bounded on $[0, \tau]$. On the other hand, a linear relationship between $D\pi/D\tau$ and $DS/D\tau$ was found in [19] in the form:

$$(3.5) \quad \frac{D\pi}{D\tau} = \exp(-\mathcal{M}) \frac{DS}{D\tau}$$

with a material constant \mathcal{M} holding both for tension and shear of AISI 316H so that [19]:

$$(3.6) \quad \mathcal{M}_{\text{tension}} \approx \mathcal{M}_{\text{shear}} \approx \mathcal{M} = 6.8645.$$

The agreement of these values with the corresponding values obtained in the case of tension as well as shear is considerable, i.e. discrepancy between $\mathcal{M}_{\text{tension}}$ and $\mathcal{M}_{\text{shear}}$ amounts approximately to 0.3% at a very large range of strain rates $D\pi/D\tau \in [10^{-3}, 10^3] \text{ s}^{-1}$. Thus it is expected that \mathcal{M} is a material constant for AISI 316H. ¹⁾

If the triggering value of the invariant S (cf. (2.10)₁) where plasticity onset happens is denoted by Y , then the simplest nonlinear dependence of Y on the initial stress rate could be given by the following equation:

$$(3.7) \quad Y = Y_0 + Y_1 \left(\frac{DS(\tau)}{D\tau} \Big|_{\tau=\tau^*} \right)^m.$$

Its statical value Y_0 depends on the accumulated plastic strain accounting in such a way for the strain hardening effect. The other two quantities appearing above, namely Y_1 and m , are constants giving rise to the simplest way of nonlinear stress rate hardening.

It has been shown by experiments on AISI 316H (by means of traditional tension specimen, "bicchierino"-type specimen as well as a cruciform specimen) that the plastic stretching tensor is not perpendicular to the yield surface (cf. [3]). Taking such an evidence into account, some constitutive models have been compared and calibrated in the paper [19]. Since such a deviation from normality is not large (as relatively simple and yet general enough to be concordant with experiments) normality model introduced by Rice in [27] based on a loading function normality and generalized to tensor functions is accepted here. Similar evolution equation was derived by Ziegler from the principle of least irreversible force. Such an equation reads:

$$(3.8) \quad \mathbf{D}_P = \Lambda \left(\frac{\partial \Omega}{\partial \mathbf{S}} \right)_d.$$

This relationship has been made explicit in the papers [18, 20] in such a way to include the dependence of the loading function on the stress tensor and plastic strain as representatives of Rice's PIR (pattern of internal rearrangements). More precisely,

$$(3.9) \quad \Omega = \hat{\Omega}(\mathbf{S}, \varepsilon_P) = \tilde{\Omega}(\gamma)$$

¹⁾Instead of \mathcal{M} the value of this material constant may be more conveniently expressed (for $\tau \geq \tau^*$) by means of the integral kernel

$$J(0) \approx 1.044 \times 10^{-3} [MPa^{-1}]$$

allowing for explicit dimensions.

and stress derivatives of this function necessarily lead to the tensor generators (2.8).

On the other hand, the above consideration on the time delay of plastic yielding and dependence of the yield stress on the stress rate, allow further specialization of (3.8) by means of

$$(3.10) \quad \Lambda = \frac{DS}{D\tau} J(0) \phi(\pi).$$

The simplest evolution equation nonlinear in the stress tensor reads then (cf. (2.8)):

$$(3.11) \quad \mathbf{D}_P = \frac{DS}{D\tau} \exp(-\mathcal{M}) \eta(S - Y) \phi(\pi) (c_1 \mathbf{S}_d + c_2 (\mathbf{S}_d^2)_d),$$

where $\eta(S - Y) = 1$ for $S > Y$ and $\eta(S - Y) = 0$ otherwise (the Heaviside function), and the strain function $\phi(\pi)$ might be either unity or some function aimed to take into account the strain hardening such as:

$$\phi(\pi) = \pi^\lambda$$

where, obviously for $\lambda \neq 0$, we have a nonlinear π -dependence. Such a model with only four material constants $\{\mathcal{M}, c_1, c_2, \lambda\}$ was calibrated in [19] leading to a high correlation coefficient 0.9683 for tension and shear in the very large strain rate range $D\pi/D\tau \in [10^{-3}, 10^3] s^{-1}$. The evolution equation (3.11) may be written as follows:

$$(3.12) \quad \mathbf{D}_P = \frac{DS}{D\tau} \exp(-\mathcal{M}) \eta(S - Y) \phi(\pi) \sum_{\alpha=1}^7 \Gamma_\alpha(\gamma) \mathbf{H}_\alpha,$$

where the loading function

$$\Omega = \frac{1}{2} c_1 s_2 + \frac{1}{3} c_2 s_3$$

leads to $\Gamma_1 = c_1$, $\Gamma_2 = c_2$, $\Gamma_\alpha = 0$ ($\alpha > 2$), while the tensor generators \mathbf{H}_α ($\alpha = 1, \dots, 7$) are shown above in (2.8). Such a model could be named as *quasi-rate-independent*. This means that if we multiply (3.11) by $d\tau$, then this equation becomes incremental. However, it should be taken into account that Y depends on $DS/D\tau$ what means that time rates influence the plastic stretching tensor.

A more general rate-dependent model in its simplest form might be given by [19]

$$(3.13) \quad \mathbf{D}_P = \eta(S - Y) \phi(\pi) \sum_{\alpha=1}^7 \left(\Gamma_\alpha(\gamma) \frac{DS}{D\tau} \exp(-\mathcal{M}) + \Gamma_\alpha^\#(\gamma) \right) \mathbf{H}_\alpha$$

where, additionally $\Gamma_1^\# = c_3, \Gamma_2^\# = c_4, \Gamma_\alpha^\# = 0 (\alpha > 2)$. Necessarily, by experimental evidence, the constants c_3, c_4 must be much smaller than c_1, c_2 (cf. (3.5)). Its advantage with respect to (3.12) is that for slow processes it covers the case when the stress rate vanishes while inelastic creep strain rate is different from zero. In our considerations dealing with high strain rates it is not so important to take these additional terms into account.

4. Longitudinal plastic waves

Consider inelastic deformation in an isotropic straight cylindrical bar with circular cross-section whose longitudinal material coordinate is $\zeta \in [0, L]$ and the other material coordinates ξ, η are also Cartesian. It is assumed in the sequel that during all the considered time interval $\tau \in [0, T]$, deplanation of the cross-sections is negligible. Thus, all material points belonging initially to a normal cross section belong to the same section during all the motion. Therefore, $\zeta = \text{const}$ stands for a cross-section with such fixed material points. Moreover, it is assumed that shears are also negligible. Then the deformation gradient tensor and plastic distortion tensor have the following forms:

$$(4.1) \quad \mathbf{F} = \begin{Bmatrix} 1 + \omega & 0 & 0 \\ 0 & 1 + \omega & 0 \\ 0 & 0 & 1 + \varepsilon \end{Bmatrix},$$

$$\mathbf{F}_P = \begin{Bmatrix} (1 + \varepsilon_P)^{-1/2} & 0 & 0 \\ 0 & (1 + \varepsilon_P)^{-1/2} & 0 \\ 0 & 0 & 1 + \varepsilon_P \end{Bmatrix}.$$

Logarithmic plastic strain tensor and plastic stretching are then obtained as follows:

$$(4.2) \quad \mathbf{e}_P = \sqrt{\frac{3}{2}} \ln(1 + \varepsilon_P) \mathbf{N}, \quad \text{where } \mathbf{N} = \sqrt{\frac{1}{6}} \begin{Bmatrix} -1 & 0 & 0 \\ 0 & -1 & 0 \\ 0 & 0 & 2 \end{Bmatrix},$$

so that

$$(4.3) \quad \mathbf{D}_P = \dot{\pi} \mathbf{N} \quad \text{with} \quad \dot{\pi} \equiv \|\mathbf{D}_P\| = (\mathbf{D}_P : \mathbf{D}_P)^{1/2} = \sqrt{\frac{3}{2}} \frac{D}{D\tau} \ln(1 + \varepsilon_P).$$

In such a case of special geometry and strain conditions we have $\mathbf{D}_P = D\mathbf{e}_P/D\tau$. Of course, such a relationship would not hold in a general case. The unit tensor \mathbf{N} with the properties $\|\mathbf{N}\| = (\mathbf{N} : \mathbf{N})^{1/2} = 1$ is here introduced for convenience.

If only the longitudinal Cauchy stress component $T_{33} \equiv \sigma$ differs from zero, then from Hooke's law written with respect to the \mathcal{B}_N -configuration, i.e.

$$(4.4) \quad \mathbf{E}_E = \frac{1}{E} ((1 + \nu) \mathbf{S} - \nu \mathbf{1} \operatorname{tr} \mathbf{S})$$

(E, ν are elastic constants for isotropic body), we get the only non-zero components of the Piola-Kirchhoff tensors (2.5)₂ in the form:

$$S_{33} = E E_{E33} = \sigma (1 + \omega)^2 \frac{(1 + \varepsilon_P)^2}{1 + \varepsilon}, \quad T_{R33} = \sigma (1 + \omega)^2 = E E_{E33} \frac{1 + \varepsilon}{(1 + \varepsilon_P)^2},$$

where

$$E_{E33} = \frac{1}{2} \left(\left(\frac{1 + \varepsilon}{1 + \varepsilon_P} \right)^2 - 1 \right) \equiv \frac{1}{2} \left((1 + \varepsilon_E)^2 - 1 \right)$$

is the corresponding longitudinal elastic strain component being very small for steels ($|E_{E33}| \ll 1$). On the other hand, from $S_{11} = S_{22} = 0$ we get the lateral total stretch by means of the formula

$$(1 + \omega)^2 = \frac{1 - 2\nu E_{E33}}{1 + \varepsilon_P}.$$

The equation of balance of linear momentum written with respect to the undeformed reference configuration \mathcal{B}_0 reads:

$$(4.5) \quad \frac{\partial}{\partial \zeta} T_{R33} = \rho_0 \frac{Dv_3}{D\tau},$$

where ρ_0 is the mass density in the undeformed configuration \mathcal{B}_0 , v_3 is the longitudinal component of the velocity vector in spatial coordinates with respect to the deformed configuration \mathcal{B} , and T_{R33} is given above.

In order to complete the field equations of the problem, the following geometric relation:

$$(4.6) \quad \frac{\partial v_3}{\partial \zeta} = \frac{D\varepsilon}{D\tau},$$

is necessary. Let us introduce non-dimensional time t and non-dimensional longitudinal material coordinate Z by means of the formulae:

$$(4.7) \quad Z = \frac{\zeta}{L}, \quad t = \frac{\tau}{T},$$

such that $Z \in [0, 1]$, $t \in [0, 1]$ and $V = \frac{T}{L} v_3$ is the corresponding non-dimensional velocity.

Now, the balance law (4.5) by means of (4.6) and (4.7) may be transformed into

$$(4.8) \quad \frac{DV}{Dt} = \frac{c_0^2}{2} \frac{\partial}{\partial Z} \left(\frac{1 + \varepsilon_E}{1 + \varepsilon_P} \left((1 + \varepsilon_E)^2 - 1 \right) \right),$$

where

$$(4.9) \quad c_0^2 = \frac{E}{\rho_0} \left(\frac{T}{L} \right)^2$$

is the *non-dimensional elastic wave speed* of the linearized wave equation. Indeed, in the elastic range, $\varepsilon_P = 0$, such that (4.8) together with the following non-dimensional equation

$$(4.10) \quad \frac{\partial V}{\partial Z} = \frac{D\varepsilon}{Dt},$$

obtained from the geometric relation (4.6), give elastic wave equation. However, if plastic strain rate does not vanish, then an additional equation is necessary. Such an equation is (3.13) rewritten in its non-dimensional form. Therefore, Eqs. (4.8), (4.10) and such a transformed Eq. (3.13) are collected into the following set of nonlinear partial differential equations of the first order:

$$(4.11) \quad \frac{\partial \mathcal{U}}{\partial t} + \mathcal{A}(\mathcal{U}) \frac{\partial \mathcal{U}}{\partial Z} = \mathcal{B}^\#(\mathcal{U}),$$

where

$$(4.12) \quad \mathcal{U} = \begin{Bmatrix} V \\ \varepsilon \\ \varepsilon_P \end{Bmatrix}, \quad \mathcal{B}^\#(\mathcal{U}) = \begin{Bmatrix} 0 \\ 0 \\ \eta T b^\# \end{Bmatrix},$$

$$\mathcal{A}(\mathcal{U}) = \begin{Bmatrix} 0 & -c_0^2 a_{12} & -c_0^2 a_{13} \\ -1 & 0 & 0 \\ -\eta a_{31} & 0 & 0 \end{Bmatrix}.$$

In the above expressions for the matrix \mathcal{A} and the column-vector $\mathcal{B}^\#$, the following scalar functions are introduced:

$$2(1 + \varepsilon_P)^2 a_{12} = 3(1 + \varepsilon_E)^2 - 1, \quad (1 + \varepsilon_P)^2 a_{13} = -(1 + \varepsilon_E) \left(2(1 + \varepsilon_E)^2 - 1 \right),$$

$$(4.13) \quad a_{31} = \frac{(1 + \varepsilon_E) \mathcal{D}}{1 - (1 + \varepsilon_E)^2 \mathcal{D} \eta}, \quad \mathcal{D} = \sqrt{\frac{2}{3}} \exp(-\mathcal{M}) E \pi^\lambda (C_1 s + C_2 s^2),$$

$$b^\# = \sqrt{\frac{2}{3}} (1 + \varepsilon_P) \frac{(C_3 s + C_4 s^2) \pi^\lambda}{1 - (1 + \varepsilon_E)^2 \mathcal{D} \eta}.$$

Here the Heaviside function is denoted by $\eta = \eta(S - Y)$ and the non-dimensional second Piola-Kirchhoff stress

$$(4.14) \quad s = \frac{S_{33}}{Y_0|_{\varepsilon_P=0}} = \frac{1}{Y_0|_{\varepsilon_P=0}} EE_{E33}$$

is scaled by means of the initial yield stress at the boundary of the original (virgin) elastic range such that the reduced material constants (cf. (3.12) and (3.13)) are introduced as follows:

$$(4.15) \quad C_\alpha = \frac{c_\alpha}{Y_0|_{\varepsilon_P=0}}, \quad \alpha \in \{1, 3\} \quad \text{and} \quad C_\beta = \frac{c_\beta}{\sqrt{6} Y_0|_{\varepsilon_P=0}}, \quad \beta \in \{2, 4\}.$$

Let us assume a solution of the homogeneous part of (3.11) in the form $\mathcal{U} = \mathcal{U}_0 \exp(Z - \lambda t)$, i.e. as a wave propagating along the Z -axis at a speed $\lambda \equiv c$. With such an assumption, Eq. (4.11) is reduced to

$$(4.16) \quad (\mathcal{A} - \lambda 1) \mathcal{U}_0 = 0.$$

Since the solutions of the characteristic equation

$$(4.17) \quad \det(\mathcal{A} - \lambda 1) = -\lambda^3 + \lambda c_0^2 (a_{12} + \eta a_{13} a_{31}) = 0$$

are real and different, i.e.

$$(4.18) \quad \lambda_1 = 0, \quad \lambda_{2/3} = \pm c_0 (a_{12} + \eta a_{13} a_{31})^{1/2}$$

the wave equation is hyperbolic. It should be noted that one of the solutions vanishes.

Consider now more closely the initial elastic range characterized by $\varepsilon_P = \varepsilon_{P0} = 0$. The above solutions of (4.11) reduce for this very special case to a very simple expression for the initial nonlinear wave speed:

$$(4.19) \quad c_0^{el} = c_0 a_{12}^{1/2} = c_0 \left(1 + 3\varepsilon_E + \frac{3}{2}\varepsilon_E^2 \right)^{1/2}.$$

Of course, in this special case elastic and total strains coincide. In a subsequent elastic range characterized by means of $\varepsilon_P = \varepsilon_{P0} = \text{const} \neq 0$ we would have plastic strain-dependent *nonlinear elastic wave speed* as follows:

$$(4.20)_1 \quad c^{el} = c_0 a_{12}^{1/2} = \frac{c_0}{|1 + \varepsilon_{P0}|} \left(1 + 3\varepsilon_E + \frac{3}{2}\varepsilon_E^2 \right)^{1/2}.$$

Taking into account that for steels $|\varepsilon_E| \ll 1$, we note that in a subsequent elastic range with advanced previous plastic strains, the corresponding elastic

wave speed is predicted to be considerably smaller than the elastic wave speed in the initial elastic range. Such a proposition could serve as a basis for an experimental check of validity of the constitutive model proposed and calibrated in [19] and applied here. Concerning the character of such a wave, we see from the derivative of the elastic wave speed i.e.

$$(4.20)_2 \quad \frac{dc^{el}}{d\varepsilon} = \frac{3(1 + \varepsilon_E) c^{el}}{2(1 + 3\varepsilon_E + \frac{3}{2}\varepsilon_E^2)} > 0,$$

that an acceleration wave could be transformed into a shock wave if large elastic strains were possible. However, this cannot happen since much slower plastic wave appears immediately after a yield surface crossing.

Indeed, if $S > Y$, then plastic strain changes with time so that $\eta = \eta(S - Y) = 1$ and *plastic wave speed* c may be expressed by the following expression (cf. (4.14) and (4.18)):

$$(4.21) \quad c = c^{el} \left(1 + \frac{a_{13}a_{31}}{a_{12}} \eta \right)^{1/2} \\ = c^{el} \left(1 - \eta \frac{2(1 + \varepsilon_E)(2(1 + \varepsilon_E)^2 - 1)}{3(1 + \varepsilon_E)^2 - 1} \frac{(1 + \varepsilon_E)\mathcal{D}}{1 - (1 + \varepsilon_E)^2 \mathcal{D}\eta} \right)^{1/2}.$$

Let us note that $c < c^{el}$. For advanced plastic strains we may even neglect elastic strain in the above relationship which leads to

$$c \approx c^{el} \left(\frac{1 - 2\mathcal{D}\eta}{1 - \mathcal{D}\eta} \right)^{1/2}.$$

Thus, for a very long rod excited at one of its ends, the plastic wave front is always delayed behind an elastic precursor wave travelling with the speed c^{el} characteristic for the elastic range to which the state of material at that instant belongs.

It is worth to note that the special case of the above approximate relation when $\mathcal{D} \approx 0.5$ leads to vanishing of the plastic wave speed and this should give rise to a localization onset according to [24].

Let us now introduce left $l_{(\alpha)}$, $\alpha \in \{1, 2, 3\}$, and right $r_{(\beta)}$, $\beta \in \{1, 2, 3\}$, (column-type) eigenvectors of the Eq. (4.16) i.e.

$$(4.22) \quad l_{(\alpha)}^T (\mathcal{A}(\mathcal{U}) - \lambda_{(\alpha)} 1) = 0 \quad \text{and} \quad (\mathcal{A}(\mathcal{U}) - \lambda_{(\beta)} 1) r_{(\beta)} = 0,$$

which are orthogonal to each other i.e. $l_{(\alpha)}^T r_{(\beta)} = 0$ if $\alpha \neq \beta$. They form the

matrices

$$(4.23) \quad \begin{Bmatrix} l_{(1)}^T \\ l_{(2)}^T \\ l_{(3)}^T \end{Bmatrix} = \begin{Bmatrix} 0 & -\eta a_{31} & 1 \\ 1 & -c_0^2 a_{12}/c & -c_0^2 a_{13}/c \\ 1 & c_0^2 a_{12}/c & c_0^2 a_{13}/c \end{Bmatrix},$$

$$(4.24) \quad \{ r_{(1)} \quad r_{(2)} \quad r_{(3)} \} = \begin{Bmatrix} 0 & 1/2 & 1/2 \\ -(c_0/c)^2 a_{13} & -1/2c & 1/2c \\ (c_0/c)^2 a_{12} & -\eta a_{31}/2c & \eta a_{31}/2c \end{Bmatrix}.$$

Suppose now that instead of the material coordinate Z and time t , new coordinates r and $s \equiv t$ are introduced by means of

$$(4.25) \quad r(Z, t) = \text{const.}$$

They are *characteristics* for the *loading acceleration wave* whose front $Z = \hat{Z}(t)$ moves at the speed (cf. (4.22))

$$(4.26) \quad \frac{d\hat{Z}}{dt} = \lambda_{(2)}, \quad \lambda_{(2)} = c, \quad c = -\frac{\partial r / \partial t}{\partial r / \partial Z},$$

such that

$$(4.27) \quad (\mathcal{A}(\mathcal{U}) - \lambda_{(\alpha)} 1) \begin{bmatrix} \partial \mathcal{U} \\ \partial r \end{bmatrix} = 0 \Rightarrow \begin{bmatrix} \partial V \\ \partial r \end{bmatrix} = -c \begin{bmatrix} \partial \varepsilon \\ \partial r \end{bmatrix},$$

$$\begin{bmatrix} \partial \varepsilon_P \\ \partial r \end{bmatrix} = \eta a_{31} \begin{bmatrix} \partial \varepsilon \\ \partial r \end{bmatrix}$$

hold. In the above relationships $[\partial \mathcal{U} / \partial r]$ denotes the jump of $\partial \mathcal{U} / \partial r$ passing from one side of the characteristic (4.25) to its opposite side.

Let us transform the wave Eq. (4.11) by introducing new independent variables i.e. $\{r, t\}$ instead of $\{Z, t\}$, and multiply such a transformed equation from the left side by the corresponding left eigenvector $l_{(2)}^T$. In such a way we obtain the so-called *interior equation*

$$(4.28) \quad l_{(2)}^T \frac{\partial \mathcal{U}}{\partial t} = l_{(2)}^T \mathcal{B}^\#(\mathcal{U}),$$

which holds along each characteristic (4.25) governing the change of the solution vector \mathcal{U} along it. Obviously, the solution vector \mathcal{U} is constant along a characteristic for the quasi-rate-independent model (3.12). In other words, such a wave is

said to be *simple* (cf. [22] page 145). For the more general rate-dependent model (2.14) a change of the solution vector along a characteristic is very small since constants $\Gamma_\alpha^\# = \{c_3, c_4\}$ are much smaller than $\Gamma_\alpha = \{c_1, c_2\}$.

Let us derive an equation governing the spatial and temporal changes of $[\partial U / \partial r]$. First, transforming the wave equation from $\{Z, t\}$ to $\{r, t\}$ and differentiating such a transformed equation by r , we get

$$(4.29) \quad (\mathcal{A}(U) - c^2) \frac{\partial^2 U}{\partial r^2} \frac{\partial r}{\partial Z} + \frac{\partial \mathcal{U}^T}{\partial r^2} \frac{\partial}{\partial U} (\mathcal{A}(U) - c^2) \frac{\partial U}{\partial r} \frac{\partial r}{\partial Z} + \frac{\partial^2 U}{\partial r \partial t} = \frac{\partial \mathcal{B}^\#}{\partial U} \frac{\partial U}{\partial r}.$$

If this equation is multiplied by $l_{(2)}^T$ and the orthogonality of $l_{(\alpha)}$ and $r_{(\beta)}$ is remembered, then after taking jumps of all the terms, the above equation becomes:

$$(4.30) \quad \frac{\partial}{\partial t} \left[\frac{\partial \varepsilon}{\partial r} \right] + \mu_1 \left[\frac{\partial \varepsilon}{\partial r} \right] + \mu_2 \left[\frac{\partial \varepsilon}{\partial r} \right]^2 = 0,$$

which is the required evolution equation commonly called the *amplitude equation*. If it is solved, then jumps $[\partial V / \partial r]$ and $[\partial \varepsilon_P / \partial r]$ are easily found from (4.27). The coefficients of the amplitude equation are obtained after a tedious calculation in the following form:

$$(4.31) \quad \mu_1 = \frac{1}{2c} \left(\frac{\partial c}{\partial t} + \eta \frac{c_0^2}{c} a_{13} \frac{\partial a_{31}}{\partial t} \right) + \mu_1^\# + m^T \frac{\partial \mathcal{U}^+}{\partial r},$$

with notations:

$$\begin{aligned} \mu_1^\# &= -\frac{c_0^2}{2c^2} \eta^T a_{13} \left(\frac{\partial b^\#}{\partial \varepsilon} + a_{31} \frac{\partial b^\#}{\partial \varepsilon_P} \right), \quad m^T \equiv \{ \mu_{1V} \mu_{1\varepsilon} \mu_{1\varepsilon_P} \}, \\ \mu_{1V} &= \frac{\partial c}{\partial \varepsilon} + \eta a_{31} \frac{\partial c}{\partial \varepsilon_P} - \eta \frac{c_0^2}{c} a_{13} \left(\frac{\partial a_{31}}{\partial \varepsilon} + a_{31} \frac{\partial a_{31}}{\partial \varepsilon_P} \right), \\ \mu_{1\varepsilon} &= -\frac{\partial c}{\partial \varepsilon} + \frac{c_0^2}{c} \left(\frac{\partial a_{12}}{\partial \varepsilon} + \eta a_{31} \frac{\partial a_{13}}{\partial \varepsilon} - \eta a_{13} \frac{\partial a_{31}}{\partial \varepsilon} \right) \\ &\quad - \frac{c_0^2}{c} \left(\frac{\partial a_{12}}{\partial \varepsilon} + \eta a_{31} \frac{\partial a_{12}}{\partial \varepsilon_P} - \frac{1}{c} \left(\frac{\partial c}{\partial \varepsilon} + \eta a_{31} \frac{\partial c}{\partial \varepsilon_P} \right) \right), \\ \mu_{1\varepsilon_P} &= -\eta a_{31} \frac{\partial c}{\partial \varepsilon_P} + \eta \frac{c_0^2}{c} a_{31} \left(\frac{\partial a_{12}}{\partial \varepsilon_P} + a_{31} \frac{\partial a_{13}}{\partial \varepsilon_P} - a_{13} \frac{\partial a_{31}}{\partial \varepsilon_P} \right) \\ &\quad + \frac{c_0^2}{2c} \left(\frac{\partial a_{13}}{\partial \varepsilon} + \eta a_{31} \frac{\partial a_{13}}{\partial \varepsilon_P} - \frac{1}{c} a_{13} \left(\frac{\partial c}{\partial \varepsilon} + \eta a_{31} \frac{\partial c}{\partial \varepsilon_P} \right) \right), \end{aligned}$$

as well as

$$(4.32) \quad \mu_2 = -\frac{\partial c}{\partial \varepsilon} - \eta a_{31} \frac{\partial c}{\partial \varepsilon_P} + \frac{c_0^2}{2c} \left(\frac{\partial a_{12}}{\partial \varepsilon} + \eta a_{31} \frac{\partial a_{13}}{\partial \varepsilon_P} \right) \\ + \frac{c_0^2}{2c} \eta a_{31} \left(\frac{\partial a_{13}}{\partial \varepsilon} + \eta a_{31} \frac{\partial a_{13}}{\partial \varepsilon_P} \right) - \frac{c_0^2}{2c} \eta a_{13} \left(\frac{\partial a_{31}}{\partial \varepsilon} + \eta a_{31} \frac{\partial a_{31}}{\partial \varepsilon_P} \right).$$

The term $\mu_1^\#$ is shown separately in order to demonstrate that it vanishes for the quasi-rate-independent model (3.12). If a loading wave enters into an undisturbed region we have $\partial \mathcal{U}^+ / \partial r = 0$ so that the amplitude equation becomes significantly simplified. However, under such an assumption, caution must be observed since in front of a plastic wave there exists the corresponding elastic precursor wave.

Finally, let us remark that if the indirect wave with the speed $\lambda_{(3)} = -c$ is considered, then for such a wave $\mathcal{U} = \mathcal{U}_0 \exp(Z + c t)$ and analogous calculations with the corresponding left eigen-vector $l_{(3)}^T$ (cf. (4.18)) would give a new amplitude equation, similar to (4.30) but with other coefficients (4.31) and (4.33).

5. Numerical simulation of a Hopkinson bar

5.1. A solution algorithm and its accuracy

Consider now a Hopkinson bar as an experimental apparatus consisting of two very long and thick cylindrical coaxial elastic bars with a cylindrical, very thin and short viscoplastic cylindrical specimen (cf.[1]). The left bar is preloaded by a constant elastic tensile strain on a major part of its length such that the remaining part of the left bar is initially immobilized by a clamp which suddenly becomes broken at the beginning of the wave motion (cf. [1]). Let their material coordinates as well as time be normalized in the way shown in the previous section, i.e. by

$$(5.1) \quad t = \frac{\tau}{T}, \quad t \in [0, 1], \quad Z_k = \frac{\zeta_k}{L_k}, \quad Z_k \in [0, 1], \quad k \in \{1, 2, 3\},$$

such that their non-dimensional linearized elastic wave speeds are

$$(5.2) \quad (c_{0k}^{el})^2 = \frac{E_k}{\rho_{0k}} \left(\frac{T}{L_k} \right)^2, \quad k \in \{1, 2, 3\},$$

where indices 1,3 stand for elastic bars, and the index 2 serves to denote the tension specimen.

Boundary conditions between the bars and the specimen must include equality of normal contact forces leading to the corresponding relationships connecting their first Piola-Kirchhoff stresses. Taking into account values of the non-dimensional material and temporal coordinates t and Z_k , the boundary conditions in stresses read

$$(5.3)_1 \quad T_{R22}(0, t) = T_{R11}(1, t) \frac{A_{01}}{A_{02}} \quad \text{and} \quad T_{R33}(0, t) = T_{R22}(1, t) \frac{A_{02}}{A_{03}},$$

where A_{0k} , $k \in \{1, 2, 3\}$, are areas of undeformed cross-sections. Similarly, boundary conditions for nondimensional velocities have to take the following form:

$$(5.3)_2 \quad V_2(0, t) = V_1(1, t) \frac{L_1}{L_2} \quad \text{and} \quad V_3(0, t) = V_2(1, t) \frac{L_2}{L_3}.$$

For a numerical solution of the wave equations of the type (4.11), the following numerical method [5] is applied here. Time and material coordinates are discretized as follows:

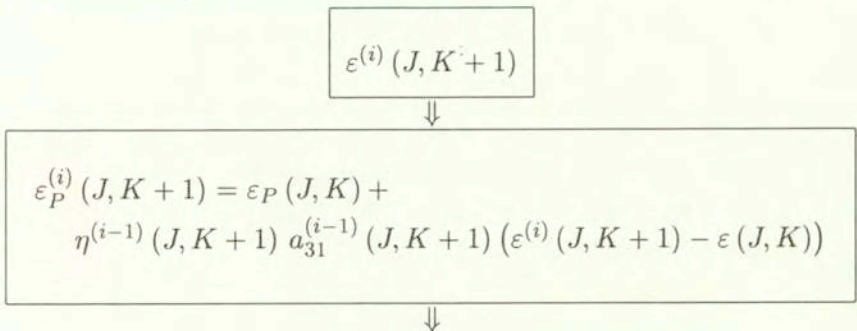
$$t \in [0, 1], \quad \Rightarrow \text{temporal index } K \in [1, M], \quad \Delta t = (M - 1)^{-1}$$

$$Z \in [0, 1], \quad \Rightarrow \text{spatial index } J \in [1, N], \quad \Delta Z = (N - 1)^{-1}$$

Implicit integration in the quasi rate-independent case (cf. (3.11)) is shown by the following scheme. Its initiation at time step $K + 1$ is determined by the last iteration values of the previous step i.e.

$$\varepsilon^{(i)}(J, K + 1) = \varepsilon(J, K)$$

with $i = 1$ at the initial iteration position and $U^{(0)}(J, K + 1) = U(J, K)$.



$$V^{(i)}(J, K+1) = V(J, K) + c_0^2 a_{12}^{(i)}(J, K+1) \partial_Z \varepsilon^{(i)}(J, K+1) \Delta t + c_0^2 a_{13}^{(i)}(J, K+1) \partial_Z \varepsilon_P^{(i)}(J, K+1) \Delta t$$

⇓

$$\partial_Z V^{(i)}(J, K+1) = 0.5 (V^{(i)}(J+1, K+1) - V^{(i)}(J-1, K+1)) / \Delta Z$$

⇓

$$\varepsilon^{(i+1)}(J, K+1) = \varepsilon(J, K) + \partial_Z V^{(i)}(J, K+1) \Delta t$$

⇓

$$ABS(\varepsilon^{(i+1)}(J, K+1) - \varepsilon^{(i)}(J, K+1)) < TOL$$

⇓
YES
⇓

$$K+1 \Leftarrow K$$

⇓
NO
⇓

$$i+1 \Leftarrow i$$

From the above algorithm we are able to derive its order of accuracy following the procedure explained in [11]. To do this we recall that (4.11) is here approximated by:

$$(5.4)_1 \quad \frac{1}{\Delta t} (\mathcal{U}_J^{K+1} - \mathcal{U}_J^K) + \frac{1}{2\Delta Z} \mathcal{A}(\mathcal{U}_J^{K+1}) (\mathcal{U}_{J+1}^{K+1} - \mathcal{U}_{J-1}^K) = \mathcal{B}^\#(\mathcal{U}_J^{K+1}).$$

Now, taking into account that the expansion of

$$(5.4)_2 \quad \mathcal{U}_{J+\beta}^{K+\alpha} \equiv \mathcal{U}(J\Delta Z + \beta\Delta Z, K\Delta t + \alpha\Delta t)$$

into power series and substitution of the obtained expression into (5.4)₁ gives the approximation of order $O(\Delta t + \Delta Z^2)$, we see that the algorithm is linear in time but it is of second order in material coordinate.

On the other hand, von Neumann stability analysis (cf. e.g. [25]) requires that $\xi < 1$ in the following solution

$$(5.4)_3 \quad \mathcal{U}_J^K = \xi^K \exp(i\chi J\Delta Z) \mathcal{U}_0$$

of (5.4)₁. Substituting (5.4)₃ into (5.4)₁ we arrive at the following form of the characteristic Eq. (4.18):

$$(5.4)_4 \quad \det \left(\mathcal{A} - i \frac{\Delta Z}{\Delta t} \frac{\xi - 1}{\xi} \frac{1}{\sin(\chi \Delta Z)} \mathcal{I} \right) = 0,$$

such that its solutions lead to the following inequality:

$$(5.4)_5 \quad \Delta t \geq \left| 1 - \frac{1}{\xi} \right| \frac{\Delta Z}{|c|} \sim \frac{\alpha_{BK} \Delta Z}{c^{el}},$$

where plastic wave speed c is determined by (4.19). Therefore, the proposed procedure is unconditionally stable permitting unbounded time increments. In the paper [6] the value $\alpha_{BK} = 5^{1/2}$ is suggested to be convenient.

Practically, for meeting some accuracy requirement by choosing $\xi \in [0.9, 1)$ we may reduce Δt as much as necessary. For instance, if the specimen is divided into 100 elements, then a convenient nondimensional time interval could be $\Delta t \sim 10^{-4}$ for the above established accuracy.

5.2. Appropriate boundary conditions

A very delicate point in this numerical routine is initialization due to the fact that geometrical changes in the apparatus are abrupt with large values of A_{01}/A_{02} as well as of L_1/L_2 . Moreover, the length of specimen is more than one hundred times smaller than lengths of the elastic bars. This means that only at the beginning of the plastic wave motion, plastic waves might be clearly recognized whereas during numerous subsequent reflections, the state of specimen strain becomes practically homogeneous.

Thus, a more realistic initialization simulating a background wave-type space-time values of velocity and strain is needed. Otherwise, a disturbance at the end of the specimen becomes numerically "frozen" and does not propagate at all along the specimen. In this paper we proceed in the following way.

For the time being, suppose that a very small disturbance of the type:

$$(5.5) \quad \varepsilon_1(0, t) = \varepsilon_0 \eta(-Z_1 + \Theta L_1), \quad \text{with } \Theta = \text{const} < 1$$

is imposed to the left (so-called "incident-reflected" bar), so that the corresponding induced strain in the specimen stays inside its initial elastic range. Here $\eta(Z) = 1$, for $Z > 0$ and $\eta(Z) = 0$ otherwise, while magnitude of ε_0 is chosen to be small enough to provoke only linear elastic wave inside the specimen due to approximately constant value of a_{12} for the wave speed c_{02}^{el} in (4.20). Then after P reflections, the incident and reflected stresses and velocities in the bars

as well as in the specimen (under the assumption of linearity of the elastic wave equation) would have the following forms:

$$(5.6) \quad \sigma_{1I} = \frac{E_1}{2} \varepsilon_0 \eta \left(t + \frac{-Z_1 + \Theta L_1}{c_{01}} \right) + \frac{E_1}{2} \varepsilon_0 \eta \left(-t + \frac{-Z_1 + \Theta L_1}{c_{01}} \right),$$

$$(5.7) \quad \sigma_{1R} = -\frac{E_1}{2} \varepsilon_0 \frac{r_{12} - 1}{r_{12} + 1} \eta \left(t + \frac{Z_1 - (1 + \Theta) L_1}{c_{01}} \right) - 2E_1 \varepsilon_0 \frac{r_{12}}{(r_{12} + 1)^2} \\ \times \frac{r_{23} - 1}{r_{23} + 1} \sum_{\alpha=1}^{P-1} (-r_{123})^{\alpha-1} \eta \left(t + \frac{Z_1 - (1 + \Theta) L_1}{c_{01}} - \frac{2\alpha L_2}{c_{02}} \right),$$

$$(5.8) \quad \sigma_{2I} = E_2 \varepsilon_0 \frac{c_{01} L_1}{c_{02} L_2} \frac{r_{12}}{r_{12} + 1} \sum_{\alpha=1}^{P-1} (-r_{123})^{\alpha-1} \\ \times \eta \left(t + \frac{Z_1 - (1 + \Theta) L_1}{c_{01}} - \frac{2\alpha L_2}{c_{02}} \right),$$

$$(5.9) \quad \sigma_{2R} = E_2 \varepsilon_0 \frac{c_{01} L_1}{c_{02} L_2} \frac{r_{12}}{r_{12} + 1} \frac{r_{23} - 1}{r_{23} + 1} \\ \times \sum_{\alpha=1}^{P-1} (-r_{123})^{\alpha-1} \eta \left(t + \frac{Z_1 - (1 + \Theta) L_1}{c_{01}} - \frac{2\alpha L_2}{c_{02}} \right),$$

$$(5.10) \quad \sigma_{3I} = 2E_3 \varepsilon_0 \frac{c_{01} L_1}{c_{03} L_3} \frac{r_{12}}{r_{12} + 1} \frac{r_{23}}{r_{23} + 1} \\ \times \sum_{\alpha=1}^{P-1} (-r_{123})^{\alpha-1} \eta \left(t - \frac{Z_3}{c_{03}} - \frac{\Theta L_1}{c_{01}} - \frac{(1 + 2\alpha) L_2}{c_{02}} \right),$$

with the following notations based on elastic impedances ²⁾

$$r_{12} = \frac{E_1 A_1}{E_2 A_2} \frac{c_{02} L_2}{c_{01} L_1}, \quad r_{23} = \frac{E_2 A_2}{E_3 A_3} \frac{c_{03} L_3}{c_{02} L_2}, \quad r_{123} = \frac{r_{12} - 1}{r_{12} + 1} \frac{r_{23} - 1}{r_{23} + 1}.$$

²⁾At the first sight, a special case of (5.8) when elastic impedance $r_{12} = 1$ leads to $r_{123} = 0$ so that σ_{2I} disappears which, obviously, is a nonsense. Such a conclusion comes from the above compact notation. In fact, when $r_{123} \rightarrow 0$, then for $\alpha = 1$ we have $\lim_{r_{123} \rightarrow 0} r_{123}^0 = 1$ so that

$$\sigma_{2I} = 0.5 E_2 \varepsilon_0 \frac{c_{01} L_1}{c_{02} L_2} \eta \left(t + \frac{Z_1 - (1 + \Theta) L_1}{c_{01}} - \frac{2L_2}{c_{02}} \right).$$

Similar result holds true for σ_{2R} and σ_{3I} given by the next two formulae, (5.9) and (5.10).

The corresponding velocities would have the values:

$$(5.11) \quad \begin{aligned} V_{1I} &= \frac{1}{2} c_{01} \varepsilon_0 \eta \left(t + \frac{-Z_1 + \Theta L_1}{c_{01}} \right) - \frac{1}{2} c_{01} \varepsilon_0 \eta \left(-t + \frac{-Z_1 + \Theta L_1}{c_{01}} \right), \\ V_{1R} &= \frac{c_{01}}{E_1} \sigma_{1R}, \quad V_{2I} = -\frac{c_{02}}{E_2} \sigma_{2I}, \quad V_{2R} = \frac{c_{02}}{E_2} \sigma_{2R}, \quad V_{3I} = -\frac{c_{03}}{E_3} \sigma_{3I}. \end{aligned}$$

Due to the assumed linearity of the elastic wave equation (which is fulfilled for very small elastic strains), the additivity condition

$$\sigma_k = \sigma_{kI} + \sigma_{kR}, \quad V_k = V_{kI} + V_{kR}$$

would hold.

5.3. Results of plastic waves inside the specimen

Let us imagine that the initial strain of the left bar, ε_0 , in (5.5)–(5.10) is now augmented enough to cause plastic straining of the specimen and that after $P = 2$, the stresses and strains in elastic bars remain unchanged. In other words, this means that during the first two reflections inside the specimen it stays inside the elastic range. Then these formulae with $P = 2$ will serve as an input into the numerical routine shown above. With this type of initiation of plastic strain of the specimen, being calculated by the proposed algorithm as a function of time and its material longitudinal coordinate, is depicted in the following figure.

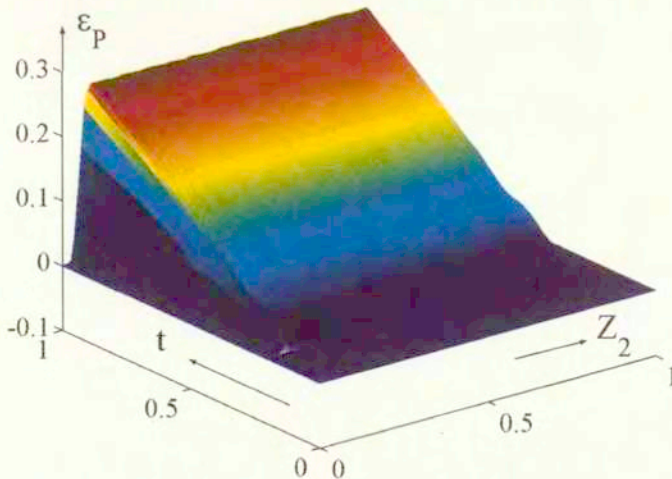


FIG. 1. Plastic wave inside the specimen as a function of space and time.

In order to underline that at initial time interval we have to deal with inhomogeneous distributions along the specimen whereas at advanced strains we

have almost constant strain along its gauge field, we show the following two figures. From the whole history, two characteristic regions are here chosen for presentation: the initial transition time interval and only the last segment of the subsequent steady time interval.

The considered example was made for the following data: $T = 0.001[s]$, $A_{01}/A_{02} = 25$, $L_1/L_2 = 250$, $E_1 = 210 \text{ GPa}$, $E_2 = 190 \text{ GPa}$, $A_{03} = A_{01}$, $L_3 = L_1$, $E_3 = E_1$, $\varepsilon_0 = 0.0016$, while ρ_0 is the mass density of steel. Taking into account the above accuracy analysis, the specimen was divided into 100 equally spaced elements. The initial time increment was taken to be slightly smaller than the corresponding Courant value [11]. The geometric transition from elastic bars to the specimen was assumed to be gradual with change of rounded corners radius in order to diminish the stress concentration [1] such that the gauge part of the specimen has two times smaller radius than its mounting ends. The initial as well as the yield stress at a non-zero plastic strain are taken respectively to be ³⁾

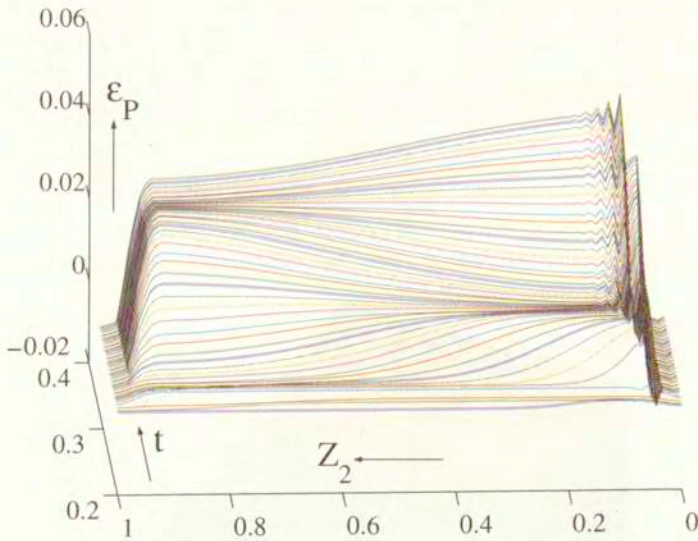


FIG. 2. Initial transition interval of plastic wave.

$$(5.12) \quad \frac{Y_0}{a} = 1 + b \left(\ln \left[\sqrt{\frac{3}{2}} E \frac{\partial \varepsilon}{\partial t} \right]_{t_0=0} \right)^c, \quad Y = Y_0 + ad\pi^e.$$

³⁾The meaning of normalizing constant a is that it is used to denote the initial yield stress at zero plastic strain and equivalent stress rate equal to $1 [MPa/s]$. The other constants appearing in (5.12) except the Young modulus as well as the "evolution" constants c_1 and c_2 are nondimensional.

These as well as material constants appearing in (3.11) are taken from [19]:

$$\begin{aligned} a &= 251.2 \text{ [MPa]}, & b &= 0.015, & c &= 1.44, & d &= 17.23, & e &= 0.5, \\ c_1 &= 1.095 \text{ [MPa}^{-1}\text{]}, & c_2 &= -0.244 \text{ [MPa}^{-2}\text{]}, & \lambda &= 0.223. \end{aligned}$$

It is worth to note that unlike (2.7), the triggering relationship (5.12) for plasticity commencement at diverse loading-unloading paths takes into account the combined strain-strain rate hardening. Thus, for strain-controlled experiments, curves $Y_0(\pi)$ are not parallel when the strain rate is varied (cf. [1, 2]).

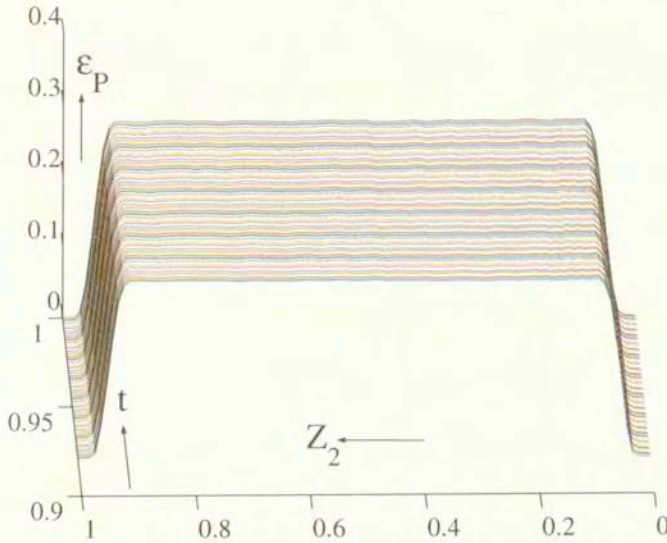


FIG. 3. Ending steady interval of plastic wave.

4.4 A discussion of Lindholm's procedure

At the end of this section, let us consider carefully the standard determination of the stress-strain state inside the specimen by means of measurements made on the elastic bars only. Suppose that two strain gauges, $SG1$ and $SG3$, are situated symmetrically at the same distance from the specimen i.e. $\vartheta L_1 = \vartheta L_3$, where $\vartheta < \Theta < 1$. In other words, $SG1$ has a position between the fixing clamp on the left (incident-reflected) bar and the left end of the specimen. Let the elastic waves in the left and the right elastic bar be:

$$u_1 = f_1 \left(t - \frac{Z_1}{c_{01}} \right) + g_1 \left(t + \frac{Z_1}{c_{01}} \right), \quad u_3 = f_3 \left(t - \frac{Z_3}{c_{03}} \right)$$

where f_1 is the *incident* wave, g_1 - the *reflected* wave and f_3 - the *transmitted* wave. Neglecting the length of the specimen we may assume that time delays at

$SG1$ and $SG3$ are approximately the same and equal to

$$\Delta t = \vartheta L_1 / c_{01} = \vartheta L_3 / c_{03}.$$

Let us denote the incident, reflected and transmitted strains by means of $\varepsilon_I(Z_1, t) = \partial f_1(\cdot) / \partial Z_1$, $\varepsilon_R(Z_1, t) = \partial g_1(\cdot) / \partial Z_1$ and $\varepsilon_T(Z_3, t) = \partial f_3(\cdot) / \partial Z_3$ respectively. Then we have

$$\begin{aligned} \varepsilon_1(1, t) &= \varepsilon_I^{SG1}(t - \Delta t) + \varepsilon_R^{SG1}(t + \Delta t) \equiv \varepsilon_I(t) + \varepsilon_R(t), \\ \varepsilon_3(0, t) &= \varepsilon_T^{SG3}(t + \Delta t) \equiv \varepsilon_T(t), \end{aligned}$$

where ε with superscripts $SG1$ and $SG3$ show readings on the strain gauges. For only two prescribed reflections caused by the augmented input ($P = 2$ in formulae (5.7)–(5.10)) as well as stresses and strains subsequently kept at fixed values, we would get the following picture for incident, reflected and transmitted strain histories at the strain gauges. Having such kind of readings as inputs, Lind-

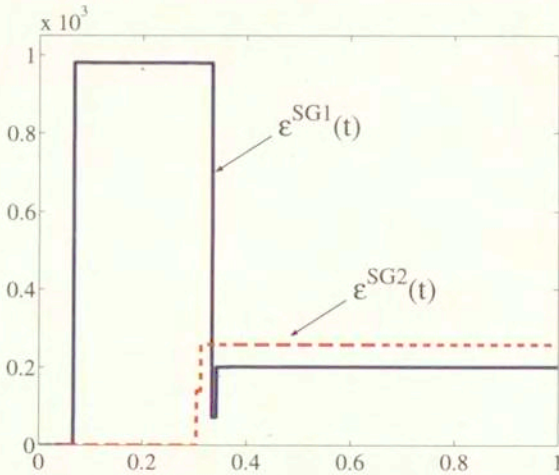


FIG. 4. Incident, reflected and transmitted strains from the left ($SG1$) and right ($SG2$) strain gages as functions of nondimensional time.

holm proposed the approximate formulae for the Cauchy stress and presumably homogeneous linear strain (cf. [12]) as follows:

$$\begin{aligned} (5.13) \quad \sigma_2(0.5, t) &\approx 0.5 (\sigma_2(0, t) + \sigma_2(1, t)) \\ &= 0.5 E_2 (A_{01} (\varepsilon_I(t) + \varepsilon_R(t)) + A_{03} \varepsilon_T(t)) / A_{02}, \end{aligned}$$

$$(5.14) \quad \varepsilon_2(0.5, t) = \frac{1}{L_2} \int_0^t (L_1 c_{01} (\varepsilon_I(t') - \varepsilon_R(t')) - L_3 c_{03} \varepsilon_T(t')) dt'.$$

Comparing the above two functions of time with the corresponding values calculated by the applied numerical routine yields the following figure which shows that Lindholm's approach should be applied with caution, having in mind that the corresponding error is considerably high. Similar conclusion, but following from some other considerations, has been drawn recently by WU and GORHAM in [29].

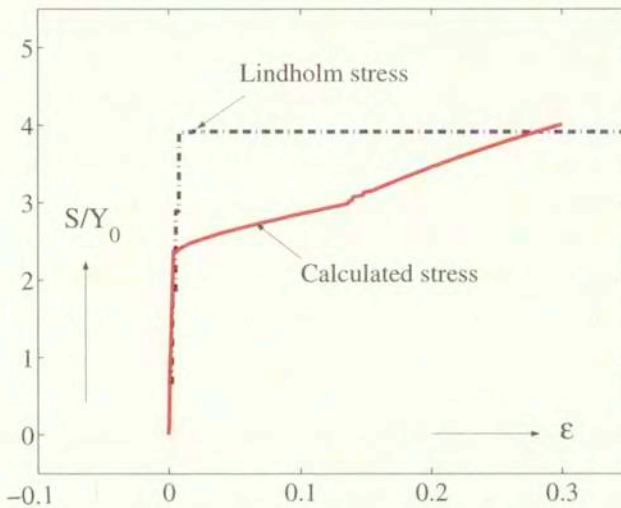


FIG. 5. Check of Lindholm's approximate formulae

6. Concluding remarks

At the end of this paper we could draw the following conclusions:

- It has been previously shown that the so-called universal flow curve and associate flow rule based on the yield function relating only scalars like equivalent stress and equivalent plastic strain was not capable of describing simultaneously the tension and shear, even in the range of only small strain rates (compare for instance [16, 19]). Although commonly used for its simplicity, such an equation is intrinsically scalar since it can describe successfully only a tension test up to large strains. The simplest yet approximately correct approach is to combine the loading function orthogonality with tensor functions.
- At present, it may be concluded that the standard Lindholm's approach to Hopkinson bar analysis does not give satisfactory answers to the assumed homogeneous stress and strain states until failure. Instead, despite the

numerical difficulties met at time and space normalization the approach which accounts explicitly for plastic waves has obvious advantages.

- It is important to underline that the flat horizontal line in the last figure follows either from the applied numerical scheme nor from the constitutive assumptions. On the contrary, boundary conditions at both ends of the specimen are assumed to fulfil Eqs. (5.5)–(5.10) dictating a fixed form of strains and stresses at the left and right end of the specimen. Then the determination of stress and strain by application of (5.13) and (5.14) necessarily lead to such a line. The point is that in such a procedure which eliminates plastic waves and reflections, the specimen is considered as a “black box”.
- However, it must be taken into account that ingenious Lindholm’s assumption has to be accepted at the beginning of a test analysis. Then, an interactive procedure should be applied to improve agreement between the theory and test, especially at the initial transition range of inelastic strains.

Acknowledgement

Research done in this paper was motivated and made possible by experimental setups and techniques developed by our friends Dr. C. Albertini and late Dr. M. Montagnani to whom our gratitude must be addressed. The authors are grateful to Prof. V. Kukudzanov for valuable comments concerning numerical solving of dynamical inelastic problems. Discussions with Prof. W. Kosiński about the subject were very helpful to us. Mr. D. Stanic made considerable effort in practical solution of the finite difference problem.

The accuracy analysis, the last two conclusions as well as the notes in the text are inserted in the revised version of the paper thanks to reviewer’s remarks.

Support of the Serbian Ministry of Science and Technology to M. M. (within grants MNTS-1309 and MNTS-0035) is gratefully acknowledged.

References

1. C. ALBERTINI and M. MONTAGNANI, *Testing techniques in dynamic biaxial loading*, Inst. Phys. Conf. Ser., **47/1**, 21–34, 1979.
2. C. ALBERTINI, M. MONTAGNANI, E. PIZZINATO and A. RODIS, *Comparison of the equivalent flow curves in tension and shear at high strain rate for AISI 316 and ARMCO iron* [in:] Proc. of Mech. Behaviour of Mater. VI, M. JONO and T. INOUE [Eds.], Pergamon, Kyoto 1991.
3. C. ALBERTINI, M. MONTAGNANI and M. MIĆUNOVIĆ, *Viscoplastic behavior of AISI 316 H: multiaxial experimental results and preliminary numerical analysis*, Nuclear Engineering and Design, **130**, 205–210, 1991.

4. C. ALBERTINI, L. J. GRIFFITHS, M. MONTAGNANI, A. RODIS, P. MARIOTTI, A. PALUFFI and G. PAZIENZA, *Material characterization by an innovative biaxial shear experiment at very large strains and at very high strain rates*, Journal de Physique IV, **1/C3**, 435-440, 1991.
5. A. BALTOV, *Investigation of dynamic processes of straining and fracture of inelastic bodies* (in Russian), Bulgarian Acad. Theoretical and Applied Mechanics, **IV/1**, Sofia 1983.
6. A. BALTOV, S. TODOROV *Application of the finite system method in the case of longitudinal bar oscillations*, Theor. Appl. Mechanics, **3**, 56-73, Sofia 1978.
7. J. KLEPACZKO, *Some experimental investigations of the elastic-plastic wave propagation in bars*, [in:] Foundations of plasticity, A. SAWCZUK [Ed.], Noordhoff Publ., Groningen 1972.
8. W. KOSIŃSKI, *Field singularities and wave analysis in continuum mechanics*, PWN, Warsaw 1986.
9. E. KRÖNER, *Allgemeine Kontinuumstheorie der Versetzungen und Eigen-spannungen*, Arch. Rational Mech. Anal., **4**, 273-334, 1970.
10. V. N. KUKUDZANOV *A numerical method for solution of nonsteady elastoviscoplastic problems at large strains*, [in:] Finite inelastic deformations - theory and applications, D. BESDO and E. STEIN [Eds.], IUTAM Proc., Springer, Berlin 1992.
11. V. N. KUKUDZANOV *Finite difference methods in solving solid mechanics problems*, (in Russian), MFTI Publications, Moscow 1992.
12. U. S. LINDHOLM, *Some experiments in dynamic plasticity under combined stress*, [in:] Symposium on the mechanical behavior of metals under dynamic loading, U. S. LINDHOLM [Ed.], San Antonio, Texas, 1967.
13. M. MIĆUNOVIĆ, *A Geometrical treatment of Thermoelasticity of simple inhomogeneous bodies: I) Geometrical and kinematical relations*, Bulletin de l'Academie Polonaise des Sciences-Serie des sciences techniques, **22/11**, 579-588, Warsaw 1974.
14. M. MIĆUNOVIĆ, C. ALBERTINI and M. MONTAGNANI, *Viscoplastic material properties at non-proportional strain histories of AISI 316 H stainless steel*. [in:] Proc. of MECAMAT, CAILLETAUD et al. [Eds.], Mecamat, Besancon 1988.
15. B. MARUSZEWSKI and M. MIĆUNOVIĆ, *On neutron irradiation of an isotropic thermo-plastic body*, Int. J. Engng. Sci., **27/8**, 955-965, 1989.
16. M. MIĆUNOVIĆ, *Normality rule from plastic work extremals?*, [in:] Proc. of CMDS-7, K H ANTHONY [Ed.], Materials Science Forum (Trans Tech Publ.), **123-125**, 609-616, 1992.
17. M. MIĆUNOVIĆ, *On viscoplasticity of irradiated steels*, **20**, J. Teor. Appl. Mech., Belgrade, 167-176, 1994.
18. M. MIĆUNOVIĆ, *Multiaxial dynamic experiments versus tensor function representation* [in:] Proc. of CMDS-8, K. Z. MARKOV [Ed.], World Scientific, 564-572, 1996.
19. M. MIĆUNOVIĆ, C. ALBERTINI and M. MONTAGNANI, *High strain rate viscoplasticity of AISI 316H stainless steel from tension and shear experiments*, [in:] Solid Mechanics, P. MILJANIC [Ed.], Serbian Acad. Sci.-Sci. Meetings, Vol. LXXXVII, Dept. Techn. Sci., **3**, 97-106, 1997.

20. M. MIĆUNOVIĆ, *On viscoplasticity of ferromagnetics*, J. Teor. Appl. Mech., **26**, 107–126, Belgrade, 2001.
21. S. MURAKAMI, *Tensor function approach to constitutive equations of inelasticity*, [in:] Transactions of SMIRT-5, A. SAWCZUK, Z. ZUDANS [Eds.], North-Holland, L., L1/4, 1979.
22. W. K. NOWACKI, *Stress waves in non-elastic solids*, Pergamon, Oxford 1978.
23. P. PERZYNA, *Fundamental problems in viscoplasticity*, Advances in Applied Mechanics, **11**, 313–387, 1971.
24. P. PERZYNA, *Interactions of elastic-viscoplastic waves and localization phenomena in solids*, [In:] Proc. IUTAM Symposium on Nonlinear Waves in Solids, J. L. WEGNER, F. R. NORWOOD [Eds.], Victoria, Canada, ASME Book No AMR137, 114–121, 1995.
25. W. H. PRESS, B. P. FLANNERY, S. A. TEUKOLSKY and W. T. VETTERLING, *Numerical recipes in C*, Cambridge Univ. Press 1990.
26. YU. N. RABOTNOV, *Elements of hereditary solid mechanics*, Mir Publishers, Moscow 1980.
27. J. R. RICE, *Inelastic constitutive relations for solids: an internal variable theory and its application to metal plasticity*, J. Mech. Phys. Solids, **19**, 433–455, 1971.
28. C. TRUESDELL and W. NOLL, *The non-linear field theories of mechanics*, [in:] Handbuch der Physik, III/3, S. FLUEGGE [Ed.], Springer, Berlin 1965.
29. X. J. WU and D. A. GORHAM, *Stress equilibrium in the split Hopkinson pressure bar test*, J. de Physique IV **7**, C3 91-96, 1997.

Received February 14, 2002; revised version April 11, 2002.
